

University of Texas Rio Grande Valley

ScholarWorks @ UTRGV

---

Chemistry Faculty Publications and  
Presentations

College of Sciences

---

10-15-2014

## Sorption of Cr(III) and Cr(VI) to High and Low Pressure Synthetic Nano-Magnetite (Fe<sub>3</sub>O<sub>4</sub>) Particles

Jason Parsons

*The University of Texas Rio Grande Valley, [jason.parsons@utrgv.edu](mailto:jason.parsons@utrgv.edu)*

Jeffrey Hernandez

Christina M. Gonzalez

J. L. Gardea-Torresdey

Follow this and additional works at: [https://scholarworks.utrgv.edu/chem\\_fac](https://scholarworks.utrgv.edu/chem_fac)

 Part of the [Chemistry Commons](#)

---

### Recommended Citation

Parsons JG, Hernandez J, Gonzalez CM, Gardea-Torresdey JL. Sorption of Cr(III) and Cr(VI) to High and Low Pressure Synthetic Nano-Magnetite (Fe<sub>3</sub>O<sub>4</sub>) Particles. *Chem Eng J.* 2014;254:171-180. doi:10.1016/j.cej.2014.05.112

This Article is brought to you for free and open access by the College of Sciences at ScholarWorks @ UTRGV. It has been accepted for inclusion in Chemistry Faculty Publications and Presentations by an authorized administrator of ScholarWorks @ UTRGV. For more information, please contact [justin.white@utrgv.edu](mailto:justin.white@utrgv.edu), [william.flores01@utrgv.edu](mailto:william.flores01@utrgv.edu).



Published in final edited form as:

*Chem Eng J.* 2014 October 15; 254: 171–180. doi:10.1016/j.cej.2014.05.112.

## Sorption of Cr(III) and Cr(VI) to High and Low Pressure Synthetic Nano-Magnetite (Fe<sub>3</sub>O<sub>4</sub>) Particles

Jason G. Parsons<sup>1,\*</sup>, Jeffrey Hernandez<sup>2</sup>, Christina M. Gonzalez<sup>2</sup>, and J. L. Gardea-Torresdey<sup>2</sup>

<sup>1</sup>Department of Chemistry, The University of Texas-Pan American 1201 W University Drive, Edinburg TX 78539, United States

<sup>2</sup>Department of Chemistry and Environmental Science and Engineering PhD program, The University of Texas at El Paso; 500 W University Ave., El Paso TX 79968, United States

### Abstract

The binding of Cr(III) and Cr(VI) to synthetic nano-magnetic particles synthesized under open vessel conditions and a microwave assisted hydrothermal synthesis techniques was investigated. Batch studies showed that the binding of both the Cr(III) and Cr(VI) bound to the nano-materials in a pH dependent manner. The Cr(III) maximized at binding at pH 4 and 100% binding. Similarly, the Cr(VI) ions showed a maximum binding of 100% at pH 4. The data from the time dependency studies showed for the most part the majority of the binding occurred within the first 5 minutes of contact with the nanomaterial and remained constant thereafter. In addition, the effects of the possible interferences were investigated which showed some effects on the binding of both Cr(III) and Cr(VI). However, the interferences never completely eliminated the chromium binding. Isotherm studies conducted at room temperature showed the microwave synthesized nanomaterials had a binding capacity of  $1208 \pm 43.9$  mg/g and  $555 \pm 10.5$  mg/g for Cr(VI) and Cr(III), respectively. However, the microwave assisted synthesized nanomaterials had capacities of  $1705 \pm 14.5$  and  $555 \pm 10.5$  mg/g for Cr(VI) and Cr(III), respectively. XANES studies showed the Cr(VI) was reduced to Cr(III), and the Cr(III) remained as Cr(III). In addition, the XANES studies indicated that the chromium remained coordinated in an octahedral arrangement of oxygen atoms.

### Keywords

Chromium(III); Chromium(VI); nano-magnetite; binding; capacity; XAS

---

© 2014 Elsevier B.V. All rights reserved.

\*Corresponding Author: phone (956)665-7462, Fax (956)665-5006, parsonsjg@utpa.edu.

**Publisher's Disclaimer:** This is a PDF file of an unedited manuscript that has been accepted for publication. As a service to our customers we are providing this early version of the manuscript. The manuscript will undergo copyediting, typesetting, and review of the resulting proof before it is published in its final citable form. Please note that during the production process errors may be discovered which could affect the content, and all legal disclaimers that apply to the journal pertain.

## Introduction

Chromium, a ubiquitous element, is found in soils, rocks and living organisms [1]. It has been used mainly in industry for its anti-corrosive properties. The plating of metals that are prone to corrosion with chromium to prevent the oxidation process [2]. Other major industrial applications include pigments, paints, and leather tanning [3]. Exposure to the chromium can cause environmental and human health problems. The different processes that are involved in making these products expose many workers to the dangerously high amounts of chromium which could lead to chromium poisoning [1]. The waste from the processes can lead to environmental pollution. The known routes of exposure to chromium include ingestion and skin absorption and inhalation [4]. Currently, the EPA has limited the amount of total chromium in drinking water to 0.100 ppm [6].

Many different methods exist to remediate heavy metals from the aqueous environment such as ion-exchange, adsorption, precipitation, co-precipitation, coagulation, and complexation. Adsorption as a method to remove Cr(VI) from the aqueous environment can be achieved through the use of iron and iron oxide based materials [7-28]. Iron oxide materials have been shown to adsorb both Cr(III) and Cr(VI) in aqueous solutions [7]. Furthermore, many iron oxide materials containing Fe<sup>2+</sup> ions have been shown to be able to reduce Cr(VI) to Cr(III) ions by transferring electrons from the Fe(II) to the Cr(VI) [8]. The sorption of Cr(VI) from solution has been studied using diatomite-supported and unsupported Magnetite particles at the micro and nanoscale. A high efficiency removal and good capacities has been observed at pHs of 11.4 and 10.6 for the supported and unsupported nano-Magnetite particles [8]. At the nanoscale the capacities were observed to be 69.2 and 21.7 mg/g for the supported and unsupported nanomagnetite particles, respectively [8]. In a similarly study montmorillonite-supported iron oxide nanoparticles showed excellent removal of Cr(VI) from aqueous solutions with a capacity of 15.5 mg/g for the supported and 10.6 mg/g for the unsupported magnetite particles [9]. Iron oxyhydroxides have been studied and have shown much promise as adsorbents, however the phases of the material has shown to have a large effect on adsorption. The synthesis conditions of many different materials has tremendous effects on the behavior of a material such as: catalytic activity, binding, as well as the surface properties, magnetic properties .

In the present study, the binding of Cr(III) and Cr(VI) to nano-magnetite was investigated to determine if the ageing process has effects on the binding properties of the nanomaterials. The nano-magnetite investigated was aged under two different conditions: a traditional heating with an open vessel and a microwave-assisted heating in a closed vessel. The nanomaterials were characterized using powder X-ray diffraction analysis. The effects of pH, time, interferences, and the binding capacity of the two materials were investigated. The interferences studied were Cl<sup>-</sup>, NO<sub>3</sub><sup>-</sup>, SO<sub>4</sub><sup>2-</sup>, and PO<sub>4</sub><sup>3-</sup> anions, which are common anions found in both surface and ground water. In addition, XANES studies were performed on the chromium bound to the nano-magnetite materials to determine the oxidation state and the coordination environment of the chromium after binding.

## Methodology

### Synthesis of iron oxide nanoparticles

The synthesis of the magnetite nanoparticles particles was performed using a method similar to that reported by Parsons et al. [11]. In brief 1.0 L of a 30 mM solution of iron(II) chloride was prepared from iron(II) chloride tetrahydrate and deionized (DI) water. The solution was then titrated with 90mL a 1.0 M solution of sodium hydroxide at a rate of approximately 0.1mL/min. The solution was maintained under constant stirring conditions to obtain a homogenous mixture. The  $\text{Fe}(\text{OH})_x$  was then placed in a Teflon vessel and heated in a Perkin Elmer Multiwave 2000 system. The particles were heated to constant temperature of 90 °C for 30 min and subsequently cooled to room temperature. The cooled samples were then centrifuged at 3000 rpm for approximately ten min and the supernatants were discarded. The particles were then dried in an oven at 100°C. The open vessel ageing process followed a similar procedure as the microwave-aged particles by heating to 90°C for 1h.

### pH study

Solution consisting of 100 ppb of either Cr(III) and Cr(VI) solutions were prepared from either chromium(III) nitrate or potassium dichromate salts, respectively. The Cr(III) and Cr(VI) solutions were pH-adjusted to 2, 3, 4, 5, and 6. The pH adjustment was performed by addition of small amounts of either HCl or NaOH under constant stirring. A mass of 10 mg of the nanomaterial were placed into 5 mL polyethylene tubes and 4.0 mL of the pH-adjusted chromium solution were added to the test tubes and equilibrated for 1hr on a rocker. Control samples were prepared for the reactions, which consisted of the chromium ions without the iron nanoparticles, in triplicate for statistical purposes. Subsequent to equilibration, the samples and controls were centrifuged at 3000 rpm for 5min and the supernatants were collected and saved for further analysis.

### Time dependency Study

10 mg samples of the nano-Magnetite particles were weighed out and placed in to a 5 mL test tube and 4 mL of the pH-adjusted (pH 4.0) Cr(III) or Cr(VI) ions were added to the test tube. The Cr(III) and Cr(VI) solution were pH adjusted to 4.0, which was determined to be the optimum binding pH. The pH adjusted samples were again equilibrated on a rocker at time intervals of 5, 10, 15, 20, 30, and 60 min. Control samples for the reactions consisted of the pH adjusted chromium solutions without the nano-Magnetite All sample and control were prepared in triplicate for statistical purposes. Subsequent to equilibration, the samples and control samples were centrifuged at 3000 rpm for 5 min and the supernatants were collected and saved for further analysis.

### Adsorption isotherm

The adsorption isotherm study was performed under a similar procedure as the pH study. The equilibration time was fixed to 1.0 h at the optimum binding pH 4 at room temperature 21°C. The Cr(III) and Cr(VI) solution concentrations used for the were 0.25, 0.50, 1.0, 5.0, and 10.0 ppm. A 10 mg sample of the nano-Magnetite was weighed out and placed into a

5.0 mL test tube and 4.0 mL aliquot of either the Cr(III) or Cr(VI) pH-adjusted solution was added. The sample was then equilibrated on a rocker to equilibrate for 1 h. Control samples consisting of the chromium solution without the nano-Magnetite. The reaction sample and control samples were prepared in triplicate for statistical purposes. Subsequent to equilibration, both the samples and controls were centrifuged at 3000 rpm for 5 min and the supernatants were collected and saved for further analysis.

### Interference study

The interfering anions used for this study were phosphate, sulfate, chloride, and nitrate, which were obtained from their sodium salts. Solutions contacting 100 ppb of either Cr(III) or Cr(VI) were prepared containing 0.1, 1.0, 10, 100 ppm of the anions. The solutions were subsequently pH-adjusted to pH 4, the optimum binding pH as previously mentioned. A 10 mg sample of the nano-Magnetite was weighed out and placed in a 5 mL test tube and a 4.0 mL aliquot of one of the pH-adjusted chromium solutions contacting one of the anions was added to the nano-Magnetite sample. The sample was then capped and placed on a rocker to equilibrate for 1 h. Controls for the reactions consisted of the chromium and anion solution without the nano-Magnetite. All reactions were performed in triplicate for statistical purposes. Subsequent to the reaction, the samples were centrifuged at 3000 rpm for 5 min and the supernatant was collected and saved for further analysis.

### GFAAS

A Perkin Elmer® Zeeman graphite furnace atomic absorption spectrometer model 5100ZL (Perkin Elmer-Shelton, CT) was used to determine the chromium concentration in solution. The calibration of the instrument was performed using a set of chromium standards prepared by serial dilution of a 1000 ppm chromium standard purchased from PlasmaCAL®. For the analysis the current for the Cr lamp was 25 mA, with a wavelength of 350 nm and a slit size of 0.7 mm. These conditions were used for all analysis. In addition, all calibration curves obtained had a  $R^2$  value of at least 0.99 or better.

### Statistical analysis

The triplicate data of the chromium solutions were analyzed with one-way analysis of variance using SPSS software, version 17.0 (SPSS Inc., Chicago, IL). Significant differences were detected using the Tukey-HSD (honestly significant difference) test. A significant difference between data points is based on a probability of  $p < 0.05$ , unless otherwise stated.

### X-ray diffraction analysis

The synthesized  $\text{Fe}_3\text{O}_4$  nanomaterials was performed using a Bruker D5000 powder X-ray diffraction. The samples were first homogenized with a mortar and pestle and placed on a platinum sample holder. The samples were diffracted from  $20\text{--}60^\circ$  in  $2\theta$  using a 8s counting time and a step of  $0.007^\circ$  at room temperature. A Le Bail fitting of the diffraction data was performed in the FullProf software to determine the phase of the material. In addition, the crystallite size of the nanoparticles was determined using Scherrer's equation and a Gaussian fitting of the diffraction data was used as well. The average grain sized was determined as an average of three independent diffraction peaks in the sample.

### XAS Sample preparation

100 ppm solutions of Cr(VI) and Cr(III) were made using reagent grade potassium dichromate ( $K_2Cr_2O_7$ ) and chromium nitrate ( $Cr(NO_3)_3$ ), respectively. These solutions were then pH-adjusted to 2, 4, and 6 using dilute sodium hydroxide and hydrochloric acid. 10 mg of either  $Fe_3O_4$  open vessel synthesized or microwave synthesized nanomaterials were weighed and put into 5mL polyethylene test tubes. Then 4mL of either of the pH adjusted Cr(III) or Cr(VI) solutions were added to the sample and equilibrated for one hour. Subsequent to equilibration the samples were centrifuged for 10 min at 3000 rpm and the solids samples were collected for analysis. This analysis was performed at Stanford Synchrotron Radiation Lightsource (SSRL, Palo Alto, CA).

### XANES study

The XANES studies were performed at SSRL on Beam Line 7-3 using a liquid helium cryostat (4-200 K). The operating conditions of the beam line were 3 GeV energy with a beam current of 50-100 mA. A Canberra 30-element array germanium detector and Si(220)  $\phi$  90 monochromator were used to obtain the Cr-K edge fluorescence spectra (Cr-K $\alpha$  5989eV). The model compounds used for comparison of the spectra were potassium dichromate and chromium (III) nitrate. A chromium foil [Cr(0)] was used as an internal calibration standard to determine the correct edge energy of each sample.

## Results and Discussion

### XRD characterization results

Figures 1 A and B show the diffraction pattern of the synthesized nanomaterials under the open vessel conditions and the microwave-assisted synthesis, respectively. As can be seen in Figures 1 A and B, the synthesized nanomaterials have the 220, 311, 222, 400, 331,422, and 511 planes observed in Magnetite [30]. The aforementioned diffraction planes correspond to the diffraction peaks located at 30.11, 35.44, 37.11, 43.11, 47.11, 53.44, and 57.00 in  $2\theta$ , respectively. It should be noted that there are two anomalous diffraction peaks, which correspond to the platinum 111 and the 220 diffraction peaks which are present from the sample holder. The platinum diffraction peaks correspond to the diffraction peaks observed at 39.44 and 45.88 in  $2\theta$ , which are indicated by the lower set of Bragg peaks in the fitting. In addition, using the Scherrer's equation, the average grain size of the nanomaterial was determined to be approximately 27 nm for the open vessel synthesis. Whereas, the average grain size of the microwave-assisted  $Fe_3O_4$  nanomaterials was approximately 25 nm. The small difference in the average grain size indicates that the ageing conditions have little to no effect on the average size of the nano-magnetite materials synthesized in this study.

### pH dependency

Figures 2 A and B show the adsorption of Cr(VI) and Cr(III) to the synthesized nanomagnetite using an open vessel synthesis and the microwave-assisted synthesis with varying pH. As can be seen in Figure 2, the binding of Cr(VI) was found to be pH dependent to both  $Fe_3O_4$  nanomaterials. At lower pH levels there were some statistical differences between pH 2 and 3; however, very little binding was shown at these low pH's. The binding

of the Cr(VI) to the microwave synthesized nano-magnetite maximized around pH 4 and remained relatively constant thereafter with no observable statistical difference at pH 5 and 6. Similarly, the binding of the Cr(VI) anions to the open vessel Fe<sub>3</sub>O<sub>4</sub> nanomaterial maximized at pH 4. However, a slight decrease in the binding of the Cr(VI) to the open vessel was observed at pH 5 and pH 6. However, the Cr(III) did not bind at low pH 2.0 very minimal binding was observed at pH 3. However, the binding increases to approximately 95-100% at pH 4 for both Fe<sub>3</sub>O<sub>4</sub> nanomaterials and remained relatively constant thereafter. Statistically differences in the binding for both nanomaterials were only observed at pH levels below 4.0. These types of trends in binding have been observed for the binding of Cr(III) and Cr(VI) to different iron nanomaterials [12,13]. For example, the percentage removal of Cr(VI) using supported/unsupported diatomite showed approximately 100% of the Cr(VI) bound [8], whereas micro-sized Magnetite particles were found to bind approximately 50% of the chromium from solution. However, the binding of the Cr(VI) was found to be stable at a low pH's from 1-3 and decreased with increasing pH up to pH 8 [8]. In a similar study using Montmorillonite-supported Magnetite nanoparticles, the authors observed high binding of Cr(VI) at a low pH and then decreased binding above pH 3. In the present study, the nano-magnetite synthesized using either the open vessel or microwave assisted technique, had similar binding trend as observed in the literature. However, slight differences in the observed binding occurred: for example the maximum binding in the literature is observed to occur at pH 3 whereas in the present study this maximum binding was observed at pH 4. In addition, the observed decrease in the binding of the Cr(VI) in occurred at slightly higher pH values of approximately 6. The overall binding trend observed for the Cr(VI) binding to the nano-magnetite had the same trends the open vessel materials had higher binding at lower pHs. The microwave-assisted synthesized Fe<sub>3</sub>O<sub>4</sub>, aged in a closed vessel, was limited in the amount of oxygen and could provide more Fe<sup>2+</sup> or some un-reacted OH<sup>-</sup> groups on the surface; whereas the ageing of the nanomaterials in the open vessel were exposed to an excess of oxygen which may have led to the formation of a layer of Fe<sup>3+</sup>, which may enhance the binding of Cr(VI) to these materials.

### Time dependency studies

Figures 3 A and B show the time dependency of the binding of both Cr(III) and Cr(VI) to the open vessel and microwave-assisted, synthesized Fe<sub>3</sub>O<sub>4</sub> nanomaterials. The Cr(VI) bound rapidly to both the open vessel and microwave-assisted synthesized nano-Magnetite, within the first five minutes of contact with the nanomaterial and remained constant thereafter. The Cr(III) reacted with the microwave-assisted synthesized Fe<sub>3</sub>O<sub>4</sub> showed a slight increase in binding as contact time increased, after 15 min the binding remained constant. The Cr(VI) binding occurred at approximately 70% and remained constant for the first 30 min and then increased up to 95 to 100 % at the one hour of contact time. Whereas the binding of the Cr(III) to the open vessel nanoparticles showed very low binding in the time ranging from 5 min to 30 min, the binding, by the 1h mark, maximized to above 90%. The binding of the Cr(VI) to the open vessel synthesized Fe<sub>3</sub>O<sub>4</sub> showed a relatively constant binding up to 30 min with a slight increase in the binding from 70% to approximately 90% between 30 and 60 min of contact time. Similarly in the literature, the time dependency of chromium binding to nanomaterials has been shown [15]. However, Cr(VI) generally requires more time to bind than Cr(III) due to different redox reactions and chemical

kinetics occurring in the reaction [15]. There are a number of examples in the literature where times of 2 and up to 24 hours are observed for maximum binding to occur. More than likely the shorter time required for binding to occur in the present study is an effect of the Cr(III) and Cr(VI) concentrations of 100ppb used in the studies. Where as in the literature concentrations of 50 to 100 ppm have been used for binding studies [8, 9, 16, 17]. The binding times observed in the present study actually represent the binding of Cr(VI) and Cr(III) to iron oxide based nanomaterials nicely. In general, the binding of Cr(VI) to iron oxide based materials shows the majority of the binding occurs within the 20-30 minutes of contact. After the first 30 minutes of contact the binding slightly increases by approximately 10-15 percent beyond what is observed in the first 30 minutes of contact [8, 9, 16, 17]

### Adsorption isotherms

Adsorption isotherms were used to determine the binding capacities for Cr(III) and Cr(VI) to the microwave and open vessel-synthesized nano-Magnetite. The isotherm data was found to fit to the Langmuir isotherm ( $R^2=0.995$ ) equation as shown below in the linearized format:

$$\frac{C_e}{Q_e} = \frac{1}{(bQ_m)} + \frac{1}{(Q_m)} C_e$$

Where  $C_e$  is the equilibrium concentration of the Cr(VI) in solution,  $b$  is a constant that is related to the ionic strength and the pH of the solution.  $Q_m$  is the capacity of the material. The capacities determined using the Langmuir equation are shown in Table 1.

This current study showed binding capacities of 0.555 mg/g and 1.705 mg/g to Cr(III) and Cr(VI) for the open vessel synthesized  $Fe_3O_4$  nanomaterial. Similar values of  $0.555 \pm 0.011$  and  $1.208 \pm 0.044$  mg/g were obtained in the reaction of Cr(III) and Cr(VI) to the microwave synthesized  $Fe_3O_4$  nanomaterial, respectively. Smith and Ghiassi found a capacity of  $9.5 \pm 0.3$  mg/g for the binding of chromate to iron(III) oxyhydroxide [16]. Smith and Ghiassi also noted that there was some co-precipitation of the chromium with the iron occurring in the reactions. The co-precipitation of the chromium was occurring through the dissolution of Fe(II) and the formation of a Cr(III)- iron complex. Yun Peng et al. [8] have investigated the removal of Cr(VI) from aqueous solutions by diatomite-supported and -unsupported magnetic nanoparticles. The researchers found that the diatomite-supported nanoparticles showed higher capacities than the unsupported nanoparticles. The observed capacities of the supported and unsupported microscale particles for the Cr(VI) were 11.4 mg/g and 10.6 mg/g, respectively. However, the nanoscale Magnetite capacities of 69.2 and 21.7 mg/g were observed for the supported and unsupported nanoparticles. The increase in the capacities of the nanomaterials, when supported, indicates that the diatomite has a high capacity for binding Cr(VI) from aqueous solution possibly due to the surface modification by the diatomite clay, which has been shown to be 11.55 mg/g [8]. A similar material,  $\gamma$ - $Fe_2O_3$  in the nanophase, has been studied for the removal of Cr(VI) from aqueous solutions at pH 2.5 [17]. The observed capacity of the  $\gamma$ - $Fe_2O_3$  nanoparticles was 15.6 mg/g. For Anatase, a titanium based material, the capacity for Cr(VI) has been observed to be 14.56 mg/g [20]. Other systems have been investigated for the removal of Cr(VI) from aqueous



solutions, such as aluminum/magnesium-mixed hydroxides which have shown capacities in the range of 105.3 to 112.0 mg/g [18]. The literature shows that  $\text{Fe}_2\text{O}_3$  has a higher binding capacity than the  $\text{Fe}_3\text{O}_4$  materials, as does  $\text{FeOOH}$ , another iron(III) compound. The preparation of nanomaterial controls their reactivity and the functionality [19]. In addition, some of the studies that show long equilibrium time and low pH's result in high chromium binding [8,9,12,13,]. In a study by Parsons et al, the adsorption of As(III) and As(V) was studied using different nanomaterials including  $\text{Fe}_3\text{O}_4$  [29]. This study showed that at low pH the iron-based nanomaterials released large amounts of iron which decreased only by increasing the pH up to pH 6 [29]. The data indicates that the high capacity observed for the binding of iron oxide nanomaterials could potentially be a co-precipitation reaction as mentioned by Smith and Ghiassi [16]. The lower capacities in the current studies may be due to the pH of reaction used in the study. The optimum binding was observed for both Cr(III) and Cr(VI) to occur at pH 4.0, whereas many of the studies performed in the literature used pH's well above this in the range of to 8, or well below pH 4.0. At pH below 4.0 iron oxides become less stable and dissolve into the solution and cause co-precipitation. Whereas at higher pH's precipitation of chromium from solution has been observed. At either pH range high binding capacities would be observed without true binding to the nanomaterial occurring.

### Interference studies

Figures 4-7 show the effects of anions that are commonly found in surface and ground water ( $\text{Cl}^-$ ,  $\text{NO}_3^-$ ,  $\text{SO}_4^{2-}$ , and  $\text{PO}_4^{3-}$ ) on the binding of Cr(VI) and Cr(III) to the open vessel and microwave-assisted synthesized nanomaterials at pH 4. The concentrations of interfering anions investigated ranged from 0.1 ppm to 100 ppm. Figures 4 A and B show the results of the interference studies with  $\text{Cl}^-$  anions. The presence of the  $\text{Cl}^-$  initially shows a small decrease in binding (approximately 10%) for the reaction between the Cr(VI) and the open vessel synthesized Magnetite. A 30% decrease in the binding of the Cr(VI) to the microwave-synthesized Magnetite was also observed. The microwave assisted synthesized Magnetite showed an initial decrease at the lower concentrations of  $\text{Cl}^-$  however the binding remains relatively constant thereafter.

Similar to the  $\text{Cl}^-$  study, the  $\text{NO}_3^-$  anion showed an initial decrease in the binding of approximately 10% and 20% for Cr(VI) binding to both the open and microwave-synthesized  $\text{Fe}_3\text{O}_4$  nanoparticles (Figures 5 A and B). The binding of Cr(VI) to the microwave-synthesized Magnetite remained constant at around 70 % with no statistical differences except the control. The open vessel magnetite showed binding around 90% with statistical differences at 0.1 and 100 ppm aside from the control. Similar results were observed for the Cr(III) and nitrate experiments as were observed in the Cr(VI) experiments. However, the Cr(III) experiments with statistical differences in the binding were observed at nitrate concentrations at 100 ppm for the microwave material . Decreased binding was observed for both the Cr(VI) and Cr(III) to the nano-Magnetite in the presence of either phosphate and sulfate anions, at low concentrations, which can be seen in Figures 6 and 7. However, at concentrations of 10 to 100 ppm of the interfering ions, interference in the binding was not observed. Also in the presence of the  $\text{SO}_4^{2-}$  and  $\text{PO}_4^{3-}$  a u-shaped curve was observed with a decrease in the binding at low concentrations of  $\text{SO}_4^{2-}$  and  $\text{PO}_4^{3-}$  as

seen in Figures 6 and 7. Statistical differences for 0.1 and 1 ppm sulfate solutions were seen for both the open and the microwave synthesized Magnetite. The same statistical difference was seen for the microwave synthesized Magnetite and the phosphate spiked Cr(VI) solution.

The Cr(III) experiment showed the same trend as the Cr(VI) experiment but at much lower binding with an increase of binding seen at higher concentrations of interference anion. A statistical difference in the Cr(III) experiment with the sulfate ion was seen at 0.1 and 1 ppm concentrations for both the microwave and open synthesis Magnetite. Similar results are shown in the literature: anions such as chloride and fluoride have little to no effect on the binding of chromate to different ion oxides [19]. The adsorption of Cr(VI) in the presence of either  $\text{SO}_4^{2-}$  or  $\text{PO}_4^{3-}$  has been shown to have reduce the binding [20]. The binding in the present study does not decrease below 50%, which indicates that there is preferential binding of the chromium to the nanomaterials compared to the interfering anions. Preferential binding is observed when one considers the mole ratios of the chromium to the anions was at the highest concentrations was as follows: Cr: $\text{Cl}^-$  1:1466, Cr: $\text{NO}_3^-$  1:838; Cr: $\text{SO}_4^{2-}$  1:541 and Cr: $\text{PO}_4^{3-}$  1:619. The u-shaped curves in the presence of  $\text{SO}_4^{2-}$  and  $\text{PO}_4^{3-}$  may be due to the potential modification of the surface by these anions, alternatively, the  $\text{SO}_4^{2-}$  and  $\text{PO}_4^{3-}$  may develop very weak buffers in solution which may affect the pH of the solution.

### XANES Study

Figure 8 A through D show the XANES spectra for the different  $\text{Fe}_3\text{O}_4$  materials, the open vessel and the hydrothermally synthesized materials after reaction with the Cr(III) and Cr(VI) ions. The prevalent characteristic in a Cr(VI) XANES spectra is the sharp peak that is located at 5989eV, known as the pre edge, due to the forbidden electron transition that occurs when the X-ray photon excites a k-shell electron which is shown in Figure 8 E for the potassium dichromate model compound. Figure A and C it can be observed that the oxidation state of the Cr that was reacted with both the micro-waved and open synthesis Magnetite nanomaterials did not remain as all Cr (VI). This change in the oxidation state can be noted by the pre edge feature in all the spectra is not characteristic of the pre edge for Cr(VI) XANES spectra, as shown in Figure 8 E for the Cr(III) nitrate model compound. The samples show that the Cr(VI) was present as a mixture of both Cr(VI) and Cr(III) bound to the nanomaterials. The spectra displayed a very small peak at the Cr(III) pre edge, which is characteristic of the Cr(III) ion. The peak did on the other hand display a sharp characteristic much like the Cr(VI) which could mean there is a relatively small amount of un-reacted Cr(VI). Much these results are similar to those obtained by White and Peterson where magnetite was observed to reduce the Cr(VI) to Cr(III) [31, 32]. In both of the Cr(III) reactions, the sample obtained from the pH 2 reaction solutions were too dilute and could not be analyzed using XANES. However, the Cr(III) bound to the magnetite nanomaterials, showed that the Cr(III) remained as Cr(III) after reaction. In addition, the data also indicates that the Cr(III) is present in an octahedral complex of oxygen atoms. The suggestion of the octahedral complex for chromium binding to the nanomaterials is from the presence of the Cr(III) pre-edge feature which has only been observed for Cr(III) bound to 6 oxygen atoms. The Cr(III) pre-edge feature shows up at approximately 5992eV(33). The Cr(III) pre-edge

feature is an allowed electronic transition of 1s electron into the 3d electron shell, and is only observed in Cr(III) that has octahedral binding to oxygen atoms.

## Conclusions

The nanomaterials bound the Cr(III) and Cr(VI) very similarly whether the nanomagnetite was synthesized and aged through microwave assisted or open vessel techniques. The pH showed similar trends in the binding of both ions to both nano-magnetite materials. The largest difference in the binding was observed in the capacity studies, the open vessel nanomaterials showed  $1.705 \pm 0.01$ , and  $0.555 \pm 2.2$  mg/g for Cr(VI) and Cr(III), respectively. The binding of the Cr(III) was found to be  $0.555 \pm 10.5$  mg/g to the microwave assisted synthesized nanomaterials. However, the Cr(VI) bonding to the microwave synthesized nanomagnetite was  $1.20 \pm 0.04$  mg/g which was a 0.5 mg/g decrease in the binding capacity compared to the open vessel synthesized nano-magnetite. Common anions,  $\text{Cl}^-$ ,  $\text{NO}_3^-$ ,  $\text{SO}_4^{2-}$  and  $\text{PO}_4^{3-}$  had varying effects on the binding of both Cr(III) and Cr(VI) to the nanomaterials. However, the binding trends for the open vessel and the microwave assisted synthesized nanomaterial show similar trends and very similar percentage binding. The XANES studies showed that the Cr(VI) was reduced to Cr(III) when bound to either the open vessel and the microwaves synthesized nano-magnetite. The reduction of the Cr(VI) to the Cr(III) occurs through the donation of electrons from the  $\text{Fe}^{2+}$  present in the  $\text{Fe}_3\text{O}_4$  materials to the chromium. In addition, it was also found that the oxidation state of the Cr(III) did not change after binding to the materials. The only observable difference in the binding between the open vessel nano-magnetite and the microwave assisted synthesized nanomaterial was the capacity for the Cr(VI).

## Acknowledgments

This material is based upon work supported by the National Science Foundation and the Environmental Protection Agency under Cooperative Agreement Number DBI-0830117. Any opinions, findings, and conclusions or recommendations expressed in this material are those of the author(s) and do not necessarily reflect the views of the National Science Foundation or the Environmental Protection Agency. This work has not been subjected to EPA review, and no official endorsement should be inferred. The authors also acknowledge USDA Grant No. 2011-38422-30835, and NSF Grant No. CHE-0840525. J.L.G.-T. acknowledges the Dudley family for the Endowed Research Professorship in Chemistry. J.G.P acknowledges NIH UTPA RISE program (Grant Number 1R25GM100866-01), NSF, URM program (grant number DBI 9034013), HHMI (grant 52007568) and financial support from the Welch Foundation for supporting the UTPA Department of Chemistry (Grant number GB-0017).

## References

1. O'Brien TJ, Ceryak S, Patierno SR. Complexities of chromium carcinogenesis: role of cellular. *Fund. Mole. Mech. Mutag.* 2003;3–36.
2. Wu Y, Zhang J, Tong Y, Xu X. Chromium (VI) reduction in aqueous solutions by  $\text{Fe}_3\text{O}_4$ -stabilized  $\text{Fe}_0$  nanoparticles. *J. Hazard. Mater.* 2009; 172:1640–1645. [PubMed: 19740609]
3. Chandra Babu NK, Asma K, Raghupathi A, Venba R, Ramesh R, Sadulla S. Screening of leather auxiliaries for their role in toxic hexavalent chromium formation in leather-posing potential health hazards to the users. *J. Clean. Prod.* 2005; 13:1189–1195.
4. Liu W, Chaspoul F, Botta C, De M eo M, Gallice P. Bioenergetics and DNA alteration of normal human fibroblasts. *Environ. Toxicol. Pharmacol.* 2009; 29:58–63. [PubMed: 21787583]
5. Franco, Rodrigo; S anchez-Olea, Roberto; Reyes-Reyes, Elsa M.; Panayiotidis, Mihalios I. Environmental toxicity, oxidative stress and apoptosis: M enage   Trois. *Mutation Research/Genetic Toxicology and Environmental Mutagenesis.* 2009; 674:3–22. 674.

6. Environmental Protection Agency. List of Contaminants & their MCLs. Jul 2. 2010 July 2010 <http://www.epa.gov/safewater/contaminants/index.html>
7. Shen YF, Tang J, Nie ZH, Wang YD, Ren Y, Zuo L. Preparation and application of magnetic Fe<sub>3</sub>O<sub>4</sub> nanoparticles for wastewater purification. *J. Sep. Purifi. Technol.* 2009; 68:312–319.
8. Yuan P, Liu D, Fan M, Yang D, Zhu R, Ge F, Zhu JX, He H. Removal of hexavalent chromium [Cr(VI)] from aqueous solutions by the diatomite-supported/unsupported Magnetite nanoparticles. *J. Hazard. Mater.* 2010; 173:614–621. [PubMed: 19748178]
9. Yuan P, Fan M, Yang D, He H, Liu D, Yuan A, Zhu JX, Chen TH. Montmorillonite-supported Magnetite nanoparticles for the removal of hexavalent chromium [Cr(VI)] from aqueous solutions. *J. Hazard. Mater.* 2009; 166:821–829. [PubMed: 19135796]
10. Wei L, Yang G, Wang R, Ma W. Selective adsorption and separation of chromium (VI) on the magnetic iron–nickel oxide from waste nickel liquid. *J. Hazard. Mater.* 2009; 164:1159–1163. [PubMed: 18954940]
11. Parsons JG, Luna C, Botez CE, Elizalde J, Gardea-Torresdey JL. Microwave-assisted synthesis of iron(III)oxyhydroxides/oxides characterized using transmission electron microscopy, X-ray diffraction, and X-ray absorption spectroscopy. *J. Phys. Chem. Solids.* 2009; 70:555–560. [PubMed: 20161181]
12. Lazaridis NK, Charalambous CH. Sorptive removal of trivalent and hexavalent chromium from binary aqueous solutions by composite alginate–goethite beads. *Water Res.* 2005; 39:4385–4396. [PubMed: 16233908]
13. Ajouyeda O, Hurel C, Ammari M, Allal LB, Marmier N. Sorption of Cr(VI) onto natural iron and aluminum (oxy)hydroxides: Effects of pH, ionic strength and initial concentration. *J. Hazard. Mater.* 2009; 174:616–622. [PubMed: 19818554]
14. Zachara JM, Girvin DC, Schmidt RL, Thomas C. Chromate adsorption on amorphous iron oxyhydroxide in the presence of major groundwater ions. *Environ. Sci. Technol.* 1987; 21:589–594. [PubMed: 19994980]
15. Gasser MS, Morad GHA, Aly HF. Batch kinetics and thermodynamics of chromium ions removal from waste solutions using synthetic adsorbents. *J. Hazard. Mater.* 2007; 142:118–129. [PubMed: 16982142]
16. Smith E, Ghiassi K. Chromate removal by an iron sorbent: mechanism and modeling. *Water Environ. Res.* 2006; 78:84–93. [PubMed: 16553170]
17. Wang P, Lo IMC. Synthesis of mesoporous magnetic  $\gamma$ -Fe<sub>2</sub>O<sub>3</sub> and its application to Cr(VI) removal from contaminated water. *Water Res.* 2009; 43:3727–3734. [PubMed: 19559458]
18. Li Y, Gao B, Wu T, Sun D, Li X, Wang B, Lu F. Hexavalent chromium removal from aqueous solution by adsorption on aluminum magnesium mixed hydroxide. *Water Res.* 2009; 43:3067–3075. [PubMed: 19439337]
19. Zhu ZL, Kong LG, Ma HM, Zhao JF. Adsorption of chromium (VI) on two iron (hydr)oxides. *Yingyong Huaxue.* 2007; 24:933–936.
20. Fukuoka H, Shigemoto N, Inomo H, Shiraki W. Chromate adsorption on iron oxyhydroxides with different crystal forms in the presence of soil materials. *J. Chem. Eng. Jap.* 2008; 41:69–75.
21. Liu JC, Huang JG. Using iron-coated spent catalyst as an alternative adsorbent to remove Cr(VI) from water. *Water Sci. Technol.* 1998; 38:155–162.
22. Mohana D, Pittman CU Jr. Activated carbons and low cost adsorbents for remediation of tri- and hexavalent chromium from water. *J. Hazard. Mater.* 2006; 137:762–811. [PubMed: 16904258]
23. Gupta VK, Rastogi A, Nayak A. Adsorption studies on the removal of hexavalent chromium from aqueous solution using a low cost fertilizer industry waste material. *J. Colloid Interface Sci.* 2010; 342:135–141. [PubMed: 19896674]
24. Sadaoui Z, Hemidouche S, Allalou O. Removal of hexavalent chromium from aqueous solutions by micellar compounds. *Desalination.* 2009; 249:768–773.
25. Magalhães F, Pereira MC, Fabris JD, Bottrel SEC, Sansiviero MTC, Amayab A, Tancredi b N, Lago RM. Novel highly reactive and regenerable carbon/iron composites prepared from tar and hematite for the reduction of Cr(VI) contaminant. *J. Hazard. Mater.* 2009; 163:1016–1022. [PubMed: 19097689]

26. Hu J, Lo IMC, Chen G. Comparative study of various magnetic nanoparticles for Cr(VI) removal. *Separ. Purif. Technol.* 2007; 56:249–256.
27. Janoš P, Hula V, Bradnová P, Pilarová V, Šedlbauer J. Reduction and immobilization of hexavalent chromium with coal- and humate-based sorbents. *Chemosphere.* 2009; 75:732–738. [PubMed: 19215962]
28. Deliyanni EA, Peleka EN, Matis KA. Modeling the sorption of metal ions from aqueous solution by iron-based adsorbents. *J. Hazard. Mater.* 2009; 172:550–558. [PubMed: 19717230]
29. Parsons JG, Lopez ML, Peralta-Videa JR, Gardea-Torresdey JL. Determination of arsenic(III) and arsenic(V) binding to microwave assisted hydrothermal synthetically prepared Fe<sub>3</sub>O<sub>4</sub>, Mn<sub>3</sub>O<sub>4</sub>, and MnFe<sub>2</sub>O<sub>4</sub> nanoadsorbents. *Microchem. J.* 2009; 91:100–106.
30. Fleet ME. The structure of Magnetite *Acta Cryst.* 1981; B37:917–920.
31. White AF, Peterson ML. Reduction of aqueous transition metal species on the surfaces of Fe(II) - containing oxides. *Geochimica et Cosmochimica Acta.* 1996; 60:3799–3814.
32. Peterson ML, Brown GE Jr, Parks GA, Stein CL. Differential redox and sorption of Cr(III/VI) on natural silicate and oxide minerals: EXAFS and XANES results. *Geochim. Cosmochim. Acta.* 1997; 61:3399–3412.
33. Parsons JG, Dokken K, Peralta-Videa JR, Romero-Gonzalez J, Gardea-Torresdey JL. X-ray absorption near edge structure and extended X-ray absorption fine structure analysis of standards and biological samples containing mixed oxidation states of chromium(III) and chromium(VI). *Appl. Spectro.* 2007; 61:338–345.

### Highlights

$\text{Fe}_3\text{O}_4$  was synthesized using two methods a microwave assisted and an open vessel.

The  $\text{Fe}_3\text{O}_4$  were in the nanometer range for both synthesis techniques

The synthesized  $\text{Fe}_3\text{O}_4$  was used for the removal of Cr ions from aqueous solution

Binding differences were observed for the materials synthesized using both techniques

Binding parameters of pH, capacity, and ionic interferences were studied.

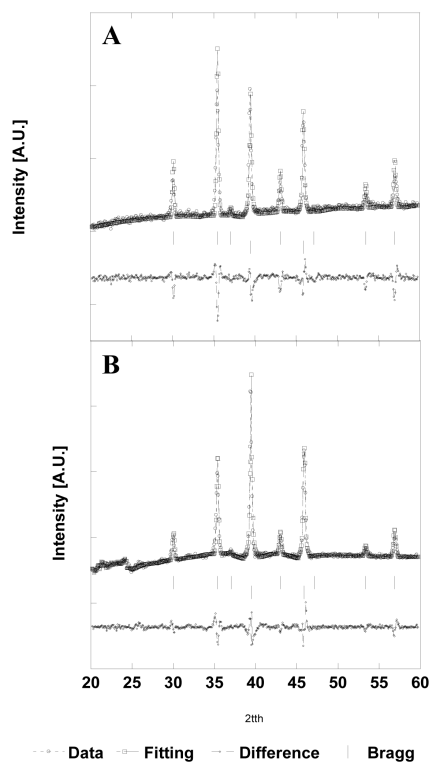


**Figure 1.** Diffraction pattern for Magnetite synthesized using open vessel synthesis protocol (A) and Magnetite synthesized using microwave synthesis protocol (B). Note Lower Bragg Peaks are from the Platinum Sample Holder.

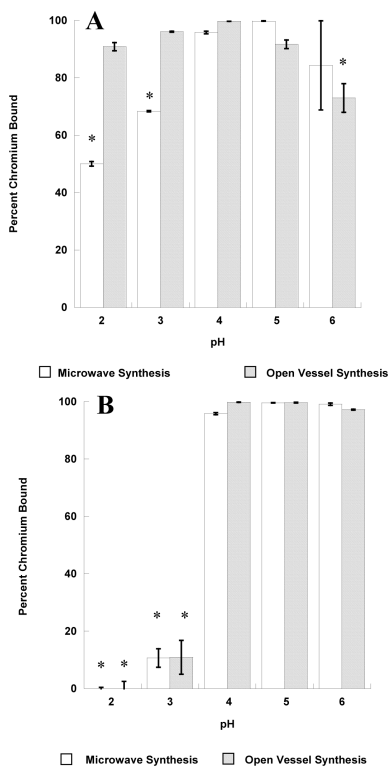


**Figure 2.**

**A.** Sorption of Cr(VI) to open and closed system synthesized nano-magnetite at pH 2-6. The error bars represent  $\pm$  standard error. \* indicate statistical differences ( $p < 0.05$ ). Comparisons were made within the microwave material (MV) and open (non-microwave) material. **B.** Sorption of Cr(III) to open and closed system synthesized nano-magnetite at pH 2-6. The error bars represent  $\pm$  standard error. \* indicate statistical differences ( $p < 0.05$ ). Comparisons were made within the microwave material (MV) and open (non-microwave) material.



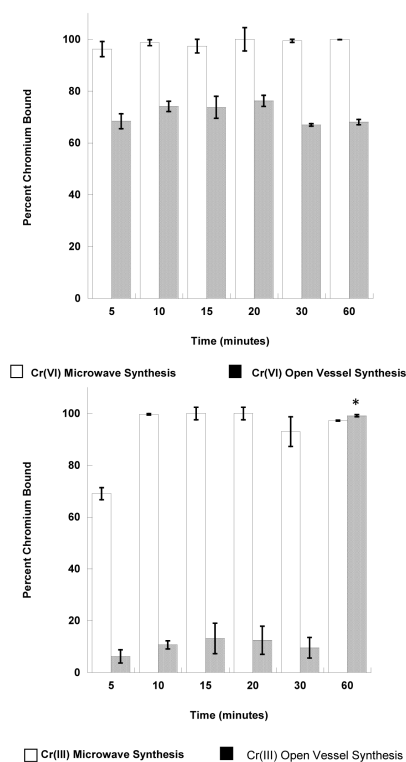


**Figure 3.**

**A.** Time dependence of Cr(VI) adsorption at a concentration of 100ppb and pH 4 to open and closed system Magnetite. Error bars represent  $\pm$  standard error. \* indicates statistical differences ( $p < 0.05$ ). Comparisons were made within the microwave material (MV) and open (non-microwave) material. **B.** Time dependence of Cr(III) adsorption at a concentration of 100ppb and pH 4 to open and closed system Magnetite. Error bars represent  $\pm$  standard error. \* indicates statistical differences ( $p < 0.05$ ). Comparisons were made within the microwave material (MV) and open (non-microwave) material.

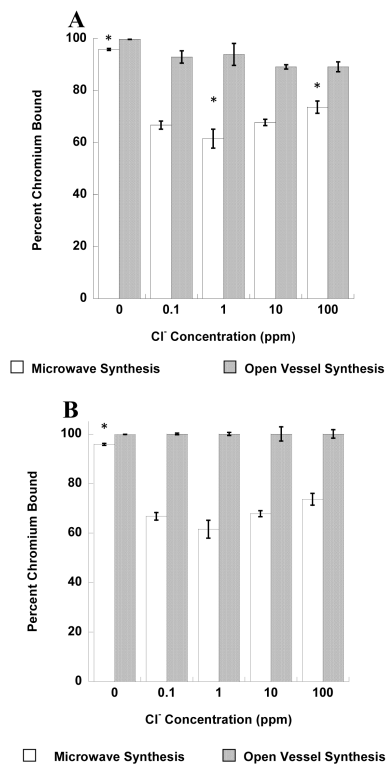


**Figure 4.** Sorption of: (A) Cr(VI) and (B) Cr(III) at 100 ppb to the Magnetite nanophase at different concentrations of chlorine anion. Error bars represent  $\pm$  standard error. \* indicates statistical differences ( $p < 0.05$ ). Comparisons were made within the microwave material (MV) and open (non-microwave) material.

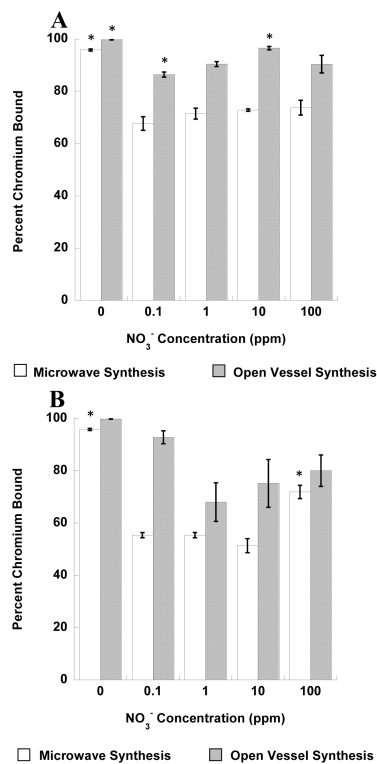


**Figure 5.** Sorption of: (A) Cr(VI) and (B) Cr(III) at 100 ppb to the Magnetite nanophase at different concentrations of nitrate anion. Error bars represent  $\pm$  standard error. \* indicates statistical differences ( $p < 0.05$ ). Comparisons were made within the microwave material (MV) and open (non-microwave) material.

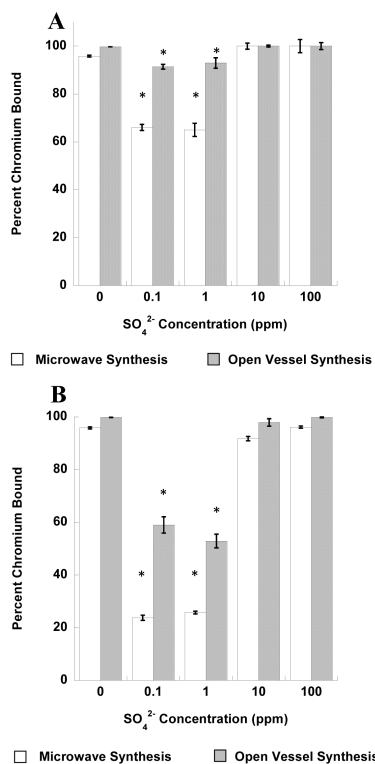


**Figure 6.**

**A.** Sorption of: **(A)** Cr(VI) and **(B)** Cr(III) at 100ppb to the Magnetite nanophase at different concentrations of sulfate anion. Error bars represent  $\pm$  standard error. \* indicates statistical differences ( $p < 0.05$ ). Comparisons were made within the microwave material (MV) and open (non-microwave) material.

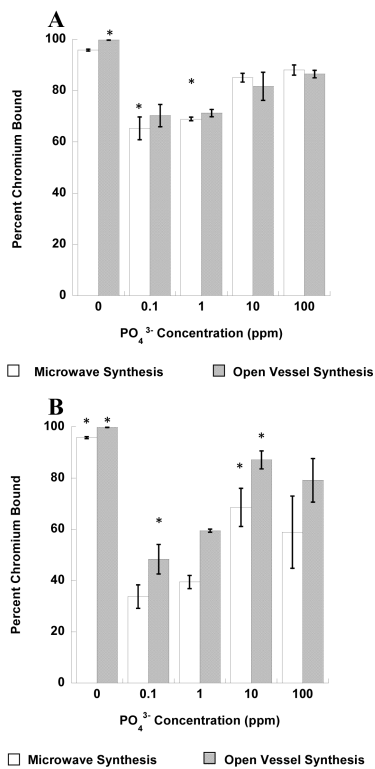


**Figure 7.** Sorption of (A) Cr(VI) and (B) Cr(III) at 100ppb to the Magnetite nanophase at different concentrations of phosphate anion. Error bars represent  $\pm$  standard error. \* indicates statistical differences ( $p < 0.05$ ). Comparisons were made within the microwave material (MV) and open (non-microwave) material

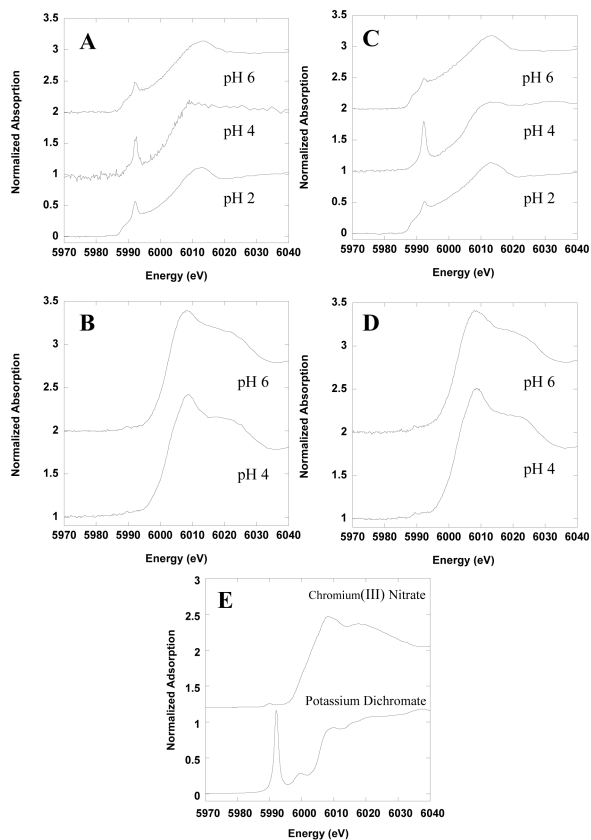


**Figure 8.** XANES spectra of Cr(VI) and Cr(III) to microwave-aged and non microwave-aged  $\text{Fe}_3\text{O}_4$ . A) Cr(VI) with MW Magnetite, B) Cr(III) with MW Magnetite, C) Cr(VI) with NMW Magnetite, D) Cr(III) with NMW Magnetite. E) Chromium(III) Nitrate and Potassium Dichromate XANES spectra.

**Table 1**

Cr(VI) and Cr(III) binding capacities based on different solution concentrations to both open and closed system nanophases

Sample	Capacity (mg/kg)	SE (+/- mg/kg)
Fe <sub>3</sub> O <sub>4</sub> Cr(VI) Microwave Synthesis	1208	43.9
Fe <sub>3</sub> O <sub>4</sub> Cr(VI) Open Vessel Synthesis	1705	14.5
Fe <sub>3</sub> O <sub>4</sub> Cr(III) Microwave Synthesis	555	10.5
Fe <sub>3</sub> O <sub>4</sub> Cr(III) Open Vessel Synthesis	555	2.2